

## 중절삭시 공구마모에 의한 절삭상태변수의 변화

장동영(서울산업대 산업공학과), Ya-Tsun Hsiao(Design Engineer, National Aerospace Fasteners Corp., Taipei, Taiwan), 김일해(서울대 기계설계학과 대학원), 김우정(서울대 기계설계학과), 한동철(서울대 기계설계학과)

### Cutting state parameter variations caused by tool wear in hard turning

Dong Young Jang(Associate Professor, Seoul National University of Technology), Ya-Tsun Hsiao(Design Engineer, National Aerospace Fasteners Corp., Taipei, Taiwan), Il Hae Kim(Ph.D. Candidate, Seoul National University), Woo Jung Kim(Research Associate, Seoul National University), Dong Chul Han(Professor, Seoul National University)

#### ABSTRACT

Machining performance in hard turning of hardened AISI M2 steel has been studied. Ceramic tools were used in the cutting tests without coolants and workpiece was prepared by heat treatment to increase its hardness up to Rc 60. Cutting state parameters such as cutting forces, temperature, and tool wear were measured in the experiments and effects of tool wear on cutting states were investigated.

**Key Words** : Hard Turning(중절삭), Tool Wear(공구마모), Surface Roughness(표면조도)

#### 1. 서론

Turning of hardened metals or "hard turning", has been popular in recent years as an economic way of generating a high quality finish on steels with a hardness of 60-65 Rc [1,2]. Compared with grinding, hard turning can machine complex workpiece in one step including steels of Rc 45 - 70 and hard power metal materials, and produce finishes approaching grinding quality. The average surface roughness (Ra) generated by hard turning is 0.2 - 0.6mm [1]. The machining cycle times of hard turning can be up to three times faster than grinding, consumes about five times less energy per metal removed than grinding, and is more environmentally friendly. It is less time consuming, more flexible, and economical.

Although grinding is the typical finishing process employed in industry, in many cases hard turning is a better option for internal and external finishing.

Many researchers [1-8] have focused their attention on hard turning process. During the cutting of hardened

steels, the temperature can reach extremes. Without coolant flooding, this high heat can be withstood by choosing right tools. Two most common insert materials for hard turning are CBN and Al<sub>2</sub>O<sub>3</sub>-TiC (aluminum-oxide titanium-carbide ceramic) for the direct heat away from the machined part surface into chips.

Since hard turning starts getting attention in machining industry recently, it is very important that production engineer is completely informed with the relationship between the characteristics of the machining process and the quality of the product.

The effect of machining on the cutting states must be understood so that remedial machining procedures can be introduced. For this purpose, cutting tests without using coolants were performed using AISI M2 tool steel in the practical ranges of cutting conditions for the hard turning operation. This steel is frequently used in manufacturing die and mold. Die and mold are usually heat-treated to increase their hardness after they are machined for their shape and dimension. Ceramic tools were used in the

experiment because of its better wear resistance in the mid-low cutting speed. The workpiece was heat-treated to increase hardness up to Rc 60.

Since heat generation in hard turning is higher and coolant is not often used, tool wear would be accelerated and cutting states parameters such as cutting forces, cutting temperature, and roughness could be easily changed over the normally acceptable limits due to the tool wear. Hence, to study variations of cutting state parameters such as surface roughness, cutting temperature, and cutting forces caused by tool wear during hard turning were conducted experimentally in this research.

## 2. HARD TURNING TESTS

A 30 horsepower engine lathe was selected for the experiment because of availability and horsepower capacity. Ceramic inserts were used to machine the workpiece. The tool insert has a small chamfer ( $20^\circ \times 0.2\text{mm}$ ) also called negative T-land on the edge and the tip radius is 0.8 mm. A tool holder held the insert. Negative rake angle ( $5^\circ$ ) was designed on the tool holder. A mechanical chip breaker was used to control the chip formation. Cutting force was measured by using a Cook Smith lathe tool dynamometer. Cutting temperature was also measured by using K-type unsheathed fine gage thermocouple with 90 cm leads.

Hardened AISI M2 high-speed steel was used as workpiece. The workpiece was cylindrical bars of 46cm long and 5.08cm diameter. To keep the uniformity of material property for five workpieces one 230 cm long steel bar was purchased and cut into five pieces. Then, five workpieces were heat treated to increase the hardness up to 60 Rc. Hardness was measured by using Rockwell hardness tester. A stopwatch was used to determine cutting time. A microscope with a video graphic printer was used to catch microscopic images of the inserts. It was set at 20 magnification. After each cut, the insert was removed from the tool holder and the average flank wear width was measured by using the microscope. The cutting tests were continued until the average flank wear reached 0.2mm. The final shape of the tool insert was pictured by using a video graphic printer. Each whole machining process was recorded by a camcorder. The schematic view of experiment setup is shown in Fig. 1.

Through modal analysis using Kistler impulsive hammer, accelerometer, and B&K Dual Channel Fast Fourier Analyzer, the dynamic characteristics of the live center-workpiece-spindle system were measured. Based

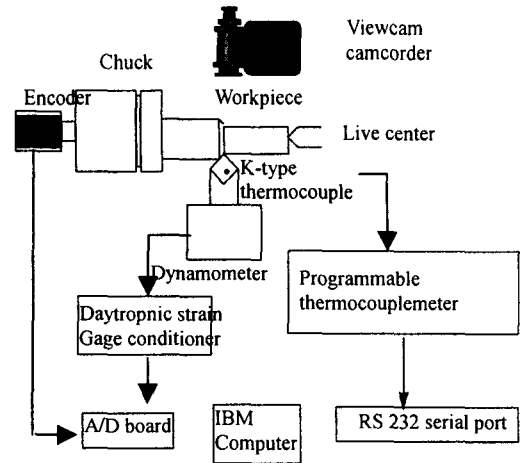


Fig. 1 Schematic view of experimental setup.

on the first mode around 160 Hz, the dynamic stability lobe was determined and limit of depth of cut was 0.4 mm of this lathe for hard turning operation. However, in order to avoid chatter, 0.3 mm of depth of cut was selected as the maximum value and cutting speed were selected between 90 m/min and 115 m/min as recommended by published papers. For finishing operation of hard turning, feed rate was varied between 0.1 mm to 0.2 mm as recommended by the tool manufacturer. The cutting conditions were summarized in Table 1.

Table 1 Cutting conditions

Cutting Conditions	Cutting Speed (m/min)	Feed rate (mm/rev)	Depth of cut (mm)
1	115	0.2	0.2
2	90	0.2	0.2
3	80	0.2	0.2
4	90	0.1	0.2
5	90	0.16	0.2
6	90	0.1	0.3
7	90	0.1	0.25

A thermocouple was embedded under the tool insert and the actual tool tip temperature was estimated through calibration using a known heat source as shown in Fig. 2. The first thermocouple was located at the tool tip while a precisely grooved carbide shim was used to hold the second thermocouple at the bottom edge of the tool insert. The relationship between two readings were determined based on the least squares curve fitting technique as follows:

$$T_{\text{edge}} = 0.873 * T_{\text{embedded}}^{1.4911}$$

### 3. RESULTS AND DISCUSSIONS

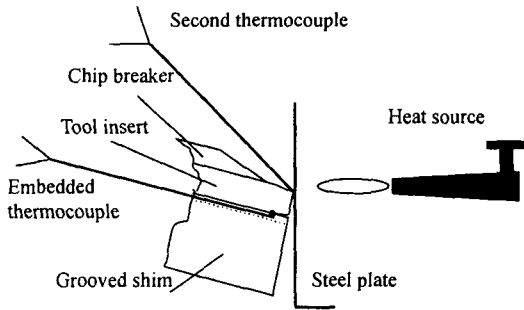


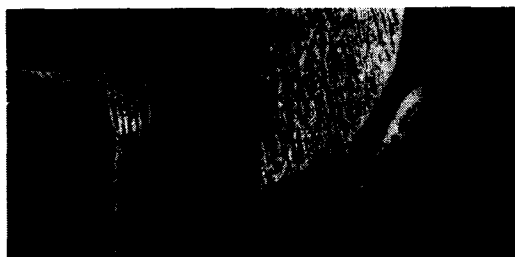
Fig. 2 Temperature calibration setup

Before the cutting tests, each bar was precut using a fresh insert to provide the similar initial condition on the workpiece. In order to prevent surface damage on the workpiece, the cutting condition of the precut was 38 m/min of cutting speed, 0.01 mm/rev of feed rate, and 0.02 mm of depth of cut. After the precut, the across-the-lay surface roughness,  $R^{\text{max}}$  along length of workpiece was measured by using the Mitutoyo surface profilometer and the outer diameters were also measured and recorded as references.  $R^{\text{max}}$  on the precut workpiece was 1.5 $\mu\text{m}$ . It was set with the cutoff length at 0.76 mm and the range at 50  $\mu\text{m}$ . The profilometer and its stand were mounted on the tool carriage of lathe so that roughness could be measured without removing the specimen from the chuck. Five measurements were conducted for each across-the-lay  $R^{\text{max}}$  and the average  $R^{\text{max}}$  with their standard deviations were recorded. The tool insert used for precut was removed from tool holder and the tool wear, if there was any, was measured and recorded. A new tool insert was used for the cutting. The cutting temperature was measured and recorded from the beginning of the cut until the end of the cut. Although cutting force was measured all the times during the cut, only several points of cutting force signals were recorded for each cut to see the cutting force variation caused by the tool wear progress. Out of three components of cutting force, only tangential component was considered for the analysis in this research since it was the biggest cutting force component and directly related to the flank wear. The whole cutting process was recorded by a camcorder. For the repeatability of tests and reliable results, cutting tests were conducted three times.

The general observation on chip formation during cutting could be described as followings. In the early cutting stages, cutting vibration, not strong as chatter was observed in all the seven cutting tests due to the high initial contact stress and low structural stiffness of the workpiece-live center side of the lathe. However, the vibration disappeared in one or two seconds during the cutting. During the cutting process, short discontinuous chips were produced at the early cutting stage and eventually changed to longer one when the tool inserts reached their wear limit. Simultaneously, the chips were burnt due to the high cutting heat and the color of them was changed from the original shiny workpiece color to the blue color for the condition #1 or brown color for the rest of cutting conditions. It might be due to the lower workpiece temperature at the beginning of cutting. Due to the high hardness, the toughness was relatively low and the chips were broken away easily. As the tool insert was reaching the tool wear limit, the cutting temperature became much higher. The cutting heat eventually changed the structure of the chips by increasing their toughness. Then, the short discontinuous chips became longer and the chip color was also changed to blue or gold. These longer discrete chips accumulated in the cutting zone and caused wear acceleration. Cutting speed had the most significant effect on chip formation due to the close relation between cutting heat and cutting speed as observed by Tönshoff [8] and Brandt [5]. Although the chip formation could indicate the progress of tool wear, it was necessary to measure the tool wear for the better tool wear prediction. The measurements of workpiece hardness before and after cutting showed that the cutting process didn't change workpiece hardness significantly.

From the observation of tool wear image using a microscope, tool wear pattern could be explained as followings. Similar wear pattern was observed in all of cutting tests. Images of worn tools for each cutting condition showed flank and crater wears in the ceramic inserts. However, the crater wear was relatively smaller and only appeared on the chamfer. Figs. 3 showed one of the microscopic image of a worn insert for condition #4. The images showed that the cutting took place on the chamfer area so that the chamfer face should be considered as the actually rake face of the tool. The average maximum depth of crater wear for all the seven tests was about 0.02 mm while the flank wear had reached its limit of 0.2 mm easily. No clear notches were

observed in all cutting tests. Therefore, flank wear would be considered as the dominant wear of ceramic tools. When depth of cut increased, the crater wear was just barely over the chamfer edge and the chipping due to thermal shock or mechanical overload was observed. These wear patterns could be explained as follows: High specific forces and high temperatures in the small contact area between tool and workpiece are dominating factors for hard turning [5-11]. During hard turning process, the welded-on chip particles could be torn off from time to time, resulting in adhesive and abrasive mechanism on flank wear [8]. As observed by Brandt [5] and Chattopadhyay [6], the accumulated chips also caused high heat accumulation in the chamfer area, resulting in superficial plastic deformation and reactional diffusion. These mechanisms might cause the acceleration of flank wear and crater wear as shown in Fig. 3.



(a) Flank wear (b) Crater wear

Fig. 3 Microscopic image of tool wear, speed = 90 m/min, feed rate = 0.1 mm/rev, depth of cut = 0.2 mm at magnification = 20

Fig. 4 showed that flank wear curves for all the cutting tests. Tests of all conditions were repeated three times for repeatability of experiments. The average flank wear width was changed more significantly by feed rate variation when feed rate effect was compared with the effect of other parameters such as cutting speed and depth of cut.

In general, the flank wear increased with increasing feed rate. For the high feed rate of 0.2 mm/rev (conditions #1, #2 and #3), the tool insert reached the wear limit in about 10 minutes. For the low feed rate of 0.1 mm/rev (conditions #4, #6 and #7), the tool life was extended a little longer. By comparing the curves of #2, #4, and #5, feed rate affected tool life as well as initial flank wear rate. The initial flank wear rate increased with the increase of feed rate. Since the initial flank wear was considered to be mainly due to the abrasion, the feed rate could be used to predict the initial abrasion rate. From the curves of #1, #2, and #3 for three different cutting

speeds, there existed a critical temperature at which the wear started being accelerated. Above that temperature, the wear increased exponentially with cutting temperature due to the high diffusion rate. The cutting speed had effect on the final stage of flank wear. Higher cutting speed eventually showed higher wear rate which might be considered to be due to the high diffusion rate. The depth of cut might also have effect on the final stage wear rate as shown in curves of #4, #6, and #7. The rate of the final stage of flank wear increased with the increase of depth of cut. However, depth of cut seemed not having strong influence on the flank wear. In general, increasing cutting speed would increase the cutting temperature exponentially and final stage of wear started as soon as the tool insert reached the critical temperature.

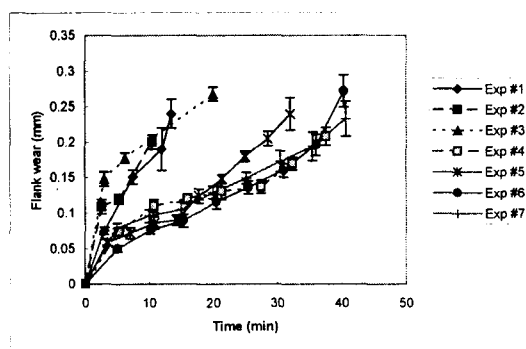


Fig. 4 Average flank wear width

Table 2 showed the cutting temperatures, surface roughness, and the cutting forces before and after tool wear, and final flank wear width when each measurement was completed for each cutting condition. This table clearly showed the effects of cutting parameters on cutting performance. Cutting temperature was directly proportional to cutting parameters such as speed, feed, and depth of cut. At the beginning of cutting, increase of cutting speed is negative effect on cutting forces and positive effect on temperature. Since the tool reached its life limit earlier for the higher cutting speed, the cutting stopped earlier for the higher cutting speed condition. Table 2 showed that in the final stage of cutting, the temperature was lower for higher cutting speed. Increase of cutting conditions caused temperatures to rise, resulting in shorter tool life.

Table 2 Cutting forces, roughness, and temperature

Case	Final flank wear Width ( $\mu\text{m}$ )	Cutting force (N)	
		New tool	Worn tool
Exp #1	240 $\pm$ 20.4	164.7 $\pm$ 7.5	262.6 $\pm$ 8.2
Exp #2	200 $\pm$ 10.5	189.7 $\pm$ 5.5	267 $\pm$ 6.7
Exp #3	270 $\pm$ 30.1	200.2 $\pm$ 8.7	276 $\pm$ 9.1
Exp #4	205 $\pm$ 12.3	124.6 $\pm$ 5.7	174.9 $\pm$ 3.3
Exp #5	246 $\pm$ 23.1	155.8 $\pm$ 4.5	217.3 $\pm$ 4.7
Exp #6	275 $\pm$ 22.8	142.4 $\pm$ 3.4	289.7 $\pm$ 8.9
Exp #7	233 $\pm$ 24.5	133.5 $\pm$ 8.3	233.2 $\pm$ 7.6

Case	Cutting Temperature ( $^{\circ}\text{C}$ )		Surface roughness $R_{\text{max}}$ ( $\mu\text{m}$ )	
	New tool	Worn tool	New tool	Worn tool
Exp #1	7.02 $\pm$ 0.15	11.02 $\pm$ 0.1	534 $\pm$ 9.1	914 $\pm$ 14.1
Exp #2	8.72 $\pm$ 0.41	11.4 $\pm$ 0.55	492 $\pm$ 8.6	966 $\pm$ 23.1
Exp #3	7 $\pm$ 0.14	8.92 $\pm$ 0.3	440 $\pm$ 8.9	1032 $\pm$ 21.2
Exp #4	3.56 $\pm$ 0.36	5.92 $\pm$ 0.3	371 $\pm$ 12.1	901 $\pm$ 4.7
Exp #5	5.92 $\pm$ 0.23	7.76 $\pm$ 0.17	453 $\pm$ 14.3	1073 $\pm$ 7.8
Exp #6	4.24 $\pm$ 0.09	7.88 $\pm$ 0.76	442 $\pm$ 6.7	1059 $\pm$ 15.4
Exp #7	4.32 $\pm$ 0.5	6.08 $\pm$ 0.27	391 $\pm$ 9.3	1072 $\pm$ 23.1

During the cutting operations, the cutting force increased due to the increase of the flank wear. It affected not only tool wear but also surface finish. In order to see the correlation between surface roughness and tool wear, the flank wear width and the average surface roughness together with its standard deviation were measured as listed in Table 2. It is well known that surface roughness is a function of tool tip radius, feed rate, tool wear, and cutting vibration. At the beginning, the effect of tool wear on the relative vibration was limited. Since the tool tip radius was held as constant, feed rate became the only factor that dominated the surface roughness. As shown in Table 2, higher feed rate eventually caused higher surface roughness. However, the effect by the relative vibration and tool wear became significant when there was enough tool wear. The surface roughness depends on feed rate, feed rate, and tool wear.

#### 4. CONCLUSIONS

In this research, cutting forces, cutting vibration, surface profiles, and tool wear were measured during hard turning of AISI M2 high speed steel by ceramic inserts. From the observations made during experiments, following conclusions can be derived

1. There was serious chip accumulation over the cutting tool when the cutting tool reached its wear limit.
2. Experiments showed that the flank wear was the dominant wear mode on the ceramic tool insert in hard turning. The crater wear was very small due

to the high resistance against chemical reaction in high temperature. Notch was unlikely to be formed.

3. Cutting only took place at chamfer area. The chamfer should be considered as the effective rake face.
4. The initial flank wear rate mainly depends on the feed rate. High feed rate eventually caused high initial flank wear rate.
5. Higher cutting speed accelerated tool wear and caused cutting temperature to rise.
6. Depth of cut was the most important cutting parameter to affect cutting force variation and the cutting force could be considered to increase due to tool wear.
7. Tool wear has direct effect on cutting state parameter variations.

#### 5. ACKNOWLEDGEMENTS

This research could be completed by the financial support from National Science Foundation of USA for their financial support (CMS 9612480) and International collaboration between Korea and USA supported by Korea Ministry of Science and Technology.

#### 참고문헌

1. D. Stovicek, Hard part turning, Tooling & Production, 57, 25-26 (1992).
2. D. Y. Jang, Y. Choi, H. Kim and A. Hsiao, Study of correlation between surface roughness and cutting vibrations to develop an on-line roughness measuring technique in hard turning, International Journal of Machine Tools & Manufacture, 36 (4), 453-464 (1996).
3. A. Carius and P. Rigby, PCBN turns the hard stuff, Cutting Tool Engineering, 47(4), 24-32 (1995).
4. P. M. Noaker, Hard turning heats up, Manufacturing Engineering, 47- 50 (1995).
5. G. Brandt, Flank and crater wear mechanisms of alumina-based cutting tools when machining steel, Wear, 112, 39-56 (1986).
6. A. K. Chattopadhyay and A. B. Chattopadhyay, Wear characteristics of ceramic cutting tools in machining steel., Wear, 110, 347-359 (1984).
7. H. Xiao, Wear behavior and wear mechanism of ceramic tools in machining hardened alloy steel, Wear, 139, 439-451 (1990).
8. H. K. Tonshoff, H. G. Wobker and D. Brandt, Tribological aspects of hard turning with ceramic tools, Lubrication Engineering, 51(2), 163-168.